Clays and Clay Minerals, Vol. 40, No. 4, 470–479, 1992.

COMPUTER SIMULATION OF CATION DISTRIBUTION IN DIOCTAHEDRAL 2:1 LAYER SILICATES USING IR-DATA: APPLICATION TO MÖSSBAUER SPECTROSCOPY OF A GLAUCONITE SAMPLE

LYDIA G. DAINYAK,[1] V. A. DRITS,[2] AND L. M. HEIFITS[3]

[1,2] Geological Institute of the Russian Academy of Science, Moscow, Russia

[3] Institute for Systems Studies of the Russian Academy of Science, Moscow, Russia

Abstract—A new approach is described to computer simulate cation distribution in octahedral sheets of dioctahedral 2:1 layer silicates with vacant trans-octahedra. This approach makes use of the information on cation distribution at the one-dimensional level provided by integrated IR optical densities for the region of OH-stretching frequencies. By using this program it is possible to show that (1) the Mössbauer spectrum of glauconite *B. Patom* conforms to the structural model composed of celandonite-like and illite-like domains whose dimensions are limited by approximately 2 or 4 unit cells; (2) non-equivalency of "left" and "right" cis-positions (with fixed b-direction) with respect to R^{2+} and R^{3+} occupancy is a characteristic feature of a celadonite-like domain.

Key Words—Cation distribution, Computer simulation, Glauconite, Mössbauer spectra.

INTRODUCTION

Analysis of the actual distribution of isomorphous cations in phyllosilicate structures is a complex problem. Diffraction methods, even if a single crystal is available, yield information only on the average composition of cation sites in the unit cell. For structurally imperfect, microdivided minerals, even these data often cannot be obtained. Spectroscopic methods are therefore especially significant since they are probes of local structure and can provide information on short-range ordering. For example, ^{29}Si MAS-NMR spectroscopy allows distinction among different tetrahedral environments of silicon (Lippmaa *et al.*, 1980; Sanz and Serratoza, 1984; Herrero *et al.*, 1987). Unfortunately, this method can be applied only to Fe-free minerals. Recently, a new deciphering procedure in IR spectra from dioctahedral micas in the region of OH-stretching frequencies has been suggested (Slonimskaya *et al.*, 1986). As a result, the integrated optical densities of the component bands assigned to different pairs of octahedral cations coordinated to the OH groups are obtained. These provide information on cation distribution at a one-dimensional level, i.e., only for one crystallographic direction.

The situation in Mössbauer spectroscopy of dioctahedral 2:1 layer silicates seems to be rather more complicated. Many authors reduce the problem of cation distribution to the Fe distribution among cis- and trans-positions. There are many papers following this concept, so we shall mention here only the more recent ones dealing with glauconite (De Grave *et al.*, 1985; Johnston and Cardile, 1987; Cardile and Brown, 1988).

At the same time, in accordance with X-ray and electron diffraction data, the trans-octahedral sites are vacant in most of 2:1 layer silicates within the limits of the method applied (Tsipursky *et al.*, 1978; Besson *et al.*, 1983; Tsipursky *et al.*, 1985; Sakharov *et al.*, 1990). We should emphasize here that interpretation of any kind of spectroscopic data for dioctahedral micas ought to be based on preliminary knowledge of cis- and trans-octahedra occupancy of the unit cell. In application to Mössbauer spectroscopy, an approach allowing for diffraction data was developed by Bookin *et al.* (1978), Dainyak *et al.* (1984a, 1984b, 1984c) and Dainyak and Drits (1987). They considered various arrangements of heterovalent cations nearest to Fe^{3+} in model systems with vacant trans-octahedra, such as nontronite, celadonite, muscovite, and ferripyrophyllite. Their approach was based on (1) crystal structure simulation methods that allowed for the size and the shape of an Fe^{3+}-octahedron as a function of the nearest neighbor cations; and (2) calculations of electric field gradients (EFG) on Fe^{3+} in terms of the ionic point-charge model. The study of model systems has shown that the problem of spectrum interpretation may have specific features in each particular case. But even if the local octahedral environments of Fe were found, the problem of reconstructing the distribution of all cation types, including Fe, would remain. Moreover, the cation distribution pattern hardly can be provided even by combination of distinct spectroscopic methods. Under the existing conditions, computer simulation would play a role as a "bridge" between the data obtained by different methods as well as between short-range and long-range order.

Computer simulation of Al-Si-distribution in tetrahedral sheets seems to be most advanced at present (Herrero *et al.*, 1987). On the other hand, simulation

of cation distribution in octahedral sheets meets with a number of difficulties. Owing to a wide variety of isomorphous substitutions, numerous alternatives may exist. Two-dimensional simulation of R^{2+}, R^{3+}, and vacancy distribution in trioctahedral mica turned out to be the simplest case (Krzanowski and Newman, 1972), provided Pauling's electroneutrality principle is applied. These authors used a computer program that suggested the possibility of extended dioctahedral fragments (domains) built within the trioctahedral matrix. At the same time this program had some shortcomings that seem to question its application to studying a real layer-silicate structure. The following shortcomings seem to be the most essential: (1) different cations having equal charges (Mg and Fe^{2+}, or Al and Fe^{3+}) are not distinguished; (2) site-by-site and row-by-row methods of filling the octahedral sheet result in chain-like domains only; and (3) numerical parameters characterizing the resultant cation distribution are absent.

Bearing in mind that IR-spectra fitting by Slonimskaya *et al.* (1986) provides concentrations of different cation pairs coordinated to the OH groups, we tried to overcome the difficulties mentioned above for the case of dioctahedral micas with vacant trans-octahedra. The results of a new computer program for simulating octahedral cation distribution have been applied to the interpretation of Mössbauer spectrum of glauconite *B. Patom.* Our aim was to find a cation distribution that would satisfy both IR and Mössbauer data.

A NEW APPROACH TO THE SIMULATION OF OCTAHEDRAL CATION DISTRIBUTION

IR data as the basis for simulation

As basic global parameters of the octahedral cation distribution, the occurrence probabilities W_{ik} (i, k = Mg, Fe^{2+}, Fe^{3+}, Al) were used. These values characterize the cation distribution between adjacent cis-octahedra linked through an OH–OH shared edge in a fixed direction. In 1 M micas, the case which is under consideration, this direction coincides with the b-axis. Integrated optical densities obtained from IR-spectroscopy are proportional to the symmetric sums of occurrence probabilities, $W_{ik} + W_{ki}$. Thus, to define occurrence probabilities properly, it is necessary to specify the degree of preference to one of the cis-positions (I and II, Figure 1) for every cation. The simplest extreme situations are: absolute preference of a cation type to one of the cis-positions, referred to as "IR-pref."; and complete absence of such preference, referred to as "IR-equiv." (An example of the analysis of such situations is considered in the following sections.) It is evident that we may optionally specify all intermediate situations.

Independent as to whether the "I" and "II" cis-octahedra are equivalent with respect to occupancies by distinct cation types, some local charge limitations may

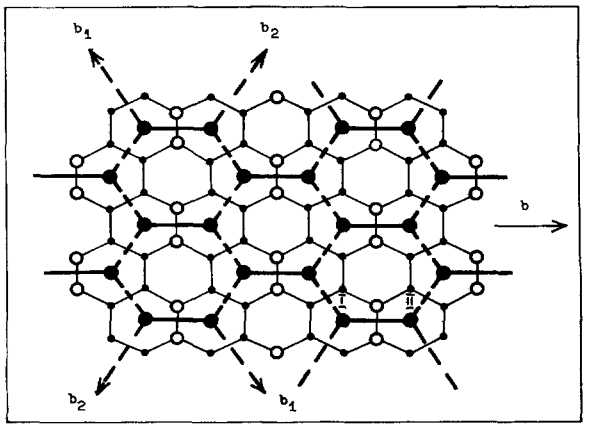

Figure 1. Honeycomb pattern of dioctahedral sheet filled with b-oriented "dumb-bells" having cations at the ends; dashed lines indicate the b_1 and b_2 directions running at $\pm 120°$ and 60° with respect to b-direction; ○ — OH, ● — O, ● — Mg, Fe^{2+}, Fe^{3+}, Al.

be imposed on the cation pair oriented along one of the directions running at $\pm 120°$, with respect to the b-direction. These directions will be hereafter referred to as b_1 and b_2 (shown by dotted lines in Figure 1). Such limitations should imply that octahedral cation distribution obeys the principle of homogeneous dispersion of charges (HDC), i.e., compensation of negative charge is approximately the same for each anion. In dioctahedral micas R^{3+} content often exceeds R^{2+} content: under HDC conditions among all possible cation pairs coordinating each anion, the $R^{3+}R^{3+}$ pairs are unavoidable, $R^{3+}R^{2+}$ pairs are preferential, and $R^{2+}R^{2+}$ pairs should be forbidden. It should be noted that $W_{R^{2+}R^{2+}}$ values are either very small or equal to zero, which follows from the results of Slonimskaya *et al.* (1986) for representative collection of micaceous minerals. Note also that the condition $W_{R^{2+}R^{2+}} = 0$ in combination with the absolute preference of R^{2+} cation to one of the cis-positions means that the HDC principle is realized.

Another kind of limitation when choosing a neighbor in the b_1 or b_2 direction may also follow from IR-data. Most IR-spectra of the minerals studied by Besson *et al.* (1987) lack an Fe^{3+} Al-band which testifies to a tendency for the segregation of Fe^{3+} and Al cations at the level of distribution along the b-axis. This tendency may be extended to cation distributions in the two-dimensional net, in b_1 and b_2 directions.

Summary of computer program

The program was developed to produce multiple random filling of a honeycomb pattern of a preset size with cation pairs, in accordance with the aforesaid limitations. Occurrence probabilities W_{ik} determine the amount of different cation pairs to be allocated in each trial. As for local limitations (HDC and segregation of

https://doi.org/10.1346/CCMN.1992.0400412 Published online by Cambridge University Press

Al and Fe^{3+} cations), in their most rigid form, it is necessary to minimize both total number of $R^{2+}R^{2+}$ pairs, N_{22}, and also the total number of $Fe^{3+}Al$ pairs, N_{FA}, appearing in lattice in directions b_1 and b_2. Clearly, the numbers of these cation pairs in the b-direction should not be considered since they are fixed by W_{ik}. Note that constraints imposed by W_{ik} may make it impossible to obtain minimal values of N_{22} and N_{FA} simultaneously. In this case (the so-called multiobjective problem) an attempt to decrease N_{22} as much as possible may increase the value of N_{FA} and vice versa. To make an explicit algorithm for lattice filling, it is necessary to define a combined, single objective function. The simplest way is to introduce a penalty function, $f(\alpha) = \alpha \cdot N_{FA} + (1 - \alpha)N_{22}$, where parameter α is to be pre-set.

The process of lattice filling is intended to obtain a cation distribution which would minimize the penalty function. Since it is impossible to implement any exact algorithm of minimization for such a complicated combinatorial situation, an heuristic algorithm was proposed. It consists of two stages. The first stage is the filling itself, and the second stage is so-called "improvement."

At the first stage cation pairs are picked up from the pool randomly, one-by-one. Then, a place is found for the chosen pair in the honeycomb lattice along the b-axis. To do this, ten possible vacant places are randomly chosen, and the best one is determined. Clearly, the best site for allocating the cation pair is the site where the pair's positioning will minimize the penalty function. The cation pair is fixed in this optimal position.

After the whole lattice has been filled, the improvement stage begins. This procedure consists of a pre-set number of steps, with an attempt at each step to exchange two randomly chosen cation pairs. If this attempt results in decreasing the penalty function, the exchange is fixed. This two-staged process seems to be satisfactory for obtaining rather random cation distribution which minimizes the penalty function.

After the process of lattice filling is completed, some numerical parameters of the cation distribution are calculated. They include: relative weights of $3R^{3+}$-, $2R^{3+}1R^{2+}$-, $2R^{2+}1R^{3+}$-, and $3R^{2+}$-arrangements consisting of three octahedral cations nearest to the central Fe^{3+}, which are relevant in Mössbauer spectroscopy; the total number of $AlFe^{3+}$ and/or $R^{2+}R^{2+}$ pairs in b_1, b_2, and b-directions that shows the effectiveness of the penalty function; the number of arrangements including three identical cations nearest to the central cation of the same sort (e.g., Al-3Al), which allows evaluation of the degree of cluster variation as undesirable cation pairs in b_1 or b_2 directions are eliminated. It should be noted that since local patterns of cation distribution cannot be adequately accounted for on the border of the lattice, the bordering cation pairs are not included in numerical parameters. After running a pre-set number of trials, the average values and standard deviations of these parameters are obtained.

We can proceed with a single lattice (number of trials is 1) to visualize the results. Any part of the filled lattice can be displayed or printed after any step of improvement procedure. This option indicates such peculiarities of the cation distribution as the shape, cation composition, and size of resulting domains varying with α and number of steps in the improvement procedure.

Thus the program considers a wide range of cation distributions with clearly formulated simulation conditions even within the limits specified by the experimental W_{ik} values (i, k = Mg, Fe^{2+}, Fe^{3+}, Al). For example, mode "IR-equiv., $\alpha = 0.5$" means that the filling of the honeycomb lattice with W_{ik} values that correspond to the equivalence of cis-positions with respect to occupancy by cations of distinct types is performed with prohibition of both $AlFe^{3+}$ and $R^{2+}R^{2+}$ in b_1 or b_2 directions. If α is 0, pairs $R^{2+}R^{2+}$ should be forbidden in b_1 or b_2 directions, and $\alpha = 1$ implies prohibition of $AlFe^{3+}$ pairs in these directions. Further on, in simulating cation distribution, we considered only the α values listed.

EXPERIMENTAL

Glauconite *B. Patom* has the composition $\{K_{0.74}Na_{0.01}Ca_{0.06}Mg_{0.06}\}[Si_{3.49}Al_{0.51}](Al_{1.15}Fe^{3+}_{0.34}Fe^{2+}_{0.20}Mg_{0.30})O_{10}(OH)_2$ calculated using the Fe^{3+}/Fe^{2+} ratio obtained from the Mössbauer spectrum. This sample was described mineralogically by Nikolaeva (1977). In accordance with X-ray and electron diffraction data, this glauconite is monomineralic and dioctahedral with vacant trans-octahedra (Kameneva, 1986).

The IR-spectrum in the region of OH-stretching frequencies was previously studied by Slonimskaya *et al.* (1986). Therefore we will not discuss the details in fitting of dioctahedral mica IR spectra, confining ourselves to the results obtained. Table 1 demonstrates integrated optical densities of individual absorption bands with corresponding frequencies (column 1).

It should be noted here that in some cases the method developed by Slonimskaya *et al.* (1986) provides the correction of the crystallo-chemical formulae of glauconites with respect to Al and Fe^{3+} distribution between tetrahedral and octahedral sites. As to the glauconite *B. Patom,* neither fitting of its IR-spectrum nor comparison of the b_{exp} parameter with the b_t parameter calculated without tetrahedral rotation (Drits *et al.,* 1992) indicates Fe^{3+} presence in tetrahedra. This is important when the initial parameters for Mössbauer spectrum fitting are specified.

The Mössbauer spectrum (Figure 2) was measured at room temperature using a $^{57}Co/Cr$ source and SM 2201 spectrometer. To eliminate the orientation effects, the sample was prepared in a hollow cone form with an approximately 55° half-cone angle (Popov *et al.,* 1988). While the absorber sample was in an in-

clined position, the absorber thickness did not exceed 7 mg Fe/cm^2.

The Mössbauer spectrum was fitted to a series of doublets. Lorentzian lineshape was assumed, and all components were assumed to have symmetric intensities and linewidths. It is well known that poor resolution of spectra inevitably yields a certain latitude in the number of doublets fitted and their parameters. In another words, statistically good fit may be achieved with various numbers of doublets and/or their parameters. The low yield of information from the fitted spectra, as well as their unsatisfactory crystallo-chemical interpretation are the consequences of this general problem. Attempts to overcome these difficulties have taken several directions: artificially increasing effective resolution of Mössbauer spectroscopy, measuring of spectra at low temperatures in an external magnetic field, and others. We use the method which includes a more or less "hard" model, assuming a certain number of doublets with *a priori* known quadrupole splittings to fit the room temperature spectrum. In the next two sections we discuss a substantiation of this model. As to the fitting program, it responds to the chosen method; namely, it supports the convergence inside the limited variation intervals for such parameters as half-width Γ, quadrupole splitting Δ, isomer shift δ and even an intensity of a component doublet. The same program may be used to synthesize spectra.

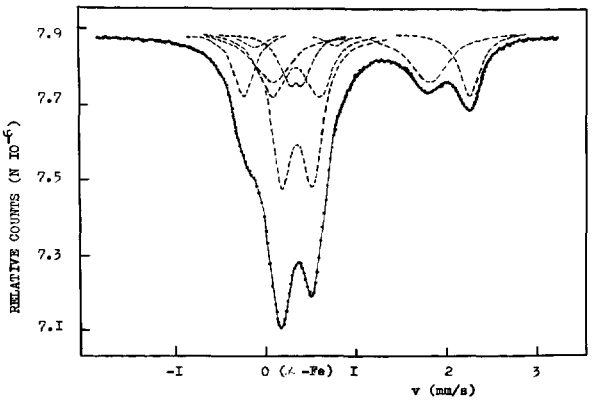

Figure 2. Mössbauer spectrum of glauconite *B. Patom* at room temperature. The fitted spectrum (dots) is calculated according to the parameters of Table 4.

RESULTS

Domain structure of glauconite B. Patom

It follows from the crystallo-chemical formula of the glauconite in question that its composition is essentially heterogeneous. At the same time the Mössbauer spectrum (Figure 2) has relatively narrow components and resembles a celadonite spectrum. Two factors interacting in the glauconite structure may be supposed to explain this peculiarity. On the one hand, the high AlAl-pair content (~40%) and the low (~8%) AlFe^{3+}-pair content (Table 1) imply a tendency for Al and Fe^{3+} segregation. On the other hand, the principle of local electrical neutrality may be obeyed where possible. If this is so, the glauconite structure may be considered as a combination of illite-like and celadonite-like domains. The same idea was used earlier for the interpretation of Mössbauer spectrum of another glauconite, but the composition of domains and the balance between them were conventional to a considerable extent (Dainyak, 1985).

If the percentage of illite- and celadonite-like domains, as it was suggested earlier (Dainyak, 1985), is determined by substitution of Al for Si in tetrahedra, then the crystallo-chemical formula of the glauconite *B. Patom* may be represented as:

$$51\%\ M^{+}_{1.0}\,[Si_{3.0}Al_{1.0}]Al_{2.0}O_{10}(OH)_2$$
$$49\%\ M^{+}_{1.0}Si_{4.0}(Al_{0.27}Fe^{3+}_{0.71}Fe^{2+}_{0.41}Mg_{0.61})O_{10}(OH)_2$$

Remembering that both of these components are present in the IR-spectrum and give absorption bands, presented in Table 1 (column 1), it is quite possible to estimate appropriate integrated optical densities. It is evident that illite-like domains should give AlAl bands only. For celadonite-like domains integrated optical densities W_{ik} should be adjusted so that the sum of cation i contributions to these bands is equal to its content, e.g.,

$$W_{Al} = (2W_{AlAl} + (W_{AlMg}) + (W_{AlFe^{2+}}) + (W_{AlFe^{3+}}).$$

Table 1. Correlation between OH-stretching frequencies and the corresponding cation pairs, and integrated optical densities of IR band (%): I - in accordance with computer-resolved IR spectrum; II - assuming 51% of illite-like domains present; III - assuming 35% of illite-like domains present.

		I	II			III		
		1	2	3	4	5	6	7
Wave number (cm^{-1})	Cation pair	Experimental data	49% of celadonite-like domain	51% of illite-like domain	Total IR-spectrum	65% of celadonite-like domain	35% of illite-like domain	Total IR-spectrum
3624 3645	AlAl	38.1	—	100.0	51.0	11.0	100.0	42.2
3607	MgAl	26.7	27.0	—	13.0	36.0	—	23.4
3589	AlFe^{3+}	8.1	—	—	—	12.0	—	7.8
3559	MgFe^{3+}	6.9	30.0	—	14.6	10.0	—	6.5
3531	Fe^{3+} Fe^{2+}	20.2	41.0	—	20.0	31.0	—	20.2
	MgMg	—	3.0	—	1.4	—	—	—

https://doi.org/10.1346/CCMN.1992.0400412 Published online by Cambridge University Press

Table 2. Occurrence probabilities of the b-oriented cation pairs W_{ik} (i,k = Mg, Fe^{2+}, Fe^{3+}, Al) in accordance with hypothetical IR-spectrum of celadonite-like domains (column 5 of Table 1): a) equivalence of cis-positions "I" and "II" with respect to cations of various types and b) preferential occupancy of one of the positions by R^{2+} cations.

a

	I				
II	Mg	Fe^{2+}	Fe^{3+}	Al	W_k
Mg	0.0	0.0	0.05	0.18	0.23
Fe^{2+}	0.0	0.0	0.16	0.0	0.16
Fe^{3+}	0.05	0.15	0.0	0.06	0.26
Al	0.18	0.0	0.06	0.11	0.35
W_i	0.23	0.15	0.27	0.35	1.0 1.0

b

	I				
II	Mg	Fe^{2+}	Fe^{3+}	Al	W_k
Mg	0.0	0.0	0.0	0.0	0.0
Fe^{2+}	0.0	0.0	0.0	0.0	0.0
Fe^{3+}	0.10	0.31	0.0	0.06	0.47
Al	0.36	0.0	0.06	0.11	0.53
W_i	0.46	0.31	0.06	0.17	1.0 1.0

Column 4 of Table 1 shows hypothetical IR-spectrum for the percentage of domains given above. It can be seen that integrated optical densities differ considerably from those obtained from the experimental IR-spectrum (column 1). If one supposes that the illite-like domains content is close to the experimental integrated optical density of AlAl band, then:

$$35\%\ M^+_1\ [Si_3Al_1]Al_2O_{10}(OH)_2$$
$$65\%\ M^+_1[Si_{3.75}Al_{0.25}](Al_{0.70}Fe^{3+}_{0.53}Fe^{2+}_{0.31}Mg_{0.46})O_{10}(OH)_2.$$

The integrated optical densities corresponding to these compositions are given in section III of Table 1. One can see that they agree well with the experiment. In this way, the data obtained from the IR-spectrum make it possible to substantiate the composition of domains, although some uncertainty as to the domain boundaries remains.

The model and the fitting of the spectrum

In terms of the supposed domain structure, the Mössbauer spectrum of the glauconite *B. Patom* is determined by celadonite-like domains, including all Fe present in the sample. Our next step in constructing the model to fit this spectrum is the synthesis of Mössbauer spectra corresponding to the various modes of cation distribution and the comparison with the experimental one. Here we make another important supposition which implies the application of point-charge calculations of the field gradient in Zavalie celadonite (Dainyak and Drits, 1987). In accordance with these calculations, the spectrum may include three Fe^{3+} doublets: the doublet with quadruple splitting (Δ) of approximately 0.17 mm/s assigned to Fe^{3+} with three nearest R^{3+} cations (arrangement $3R^{3+}$ referred to as F), the doublet with Δ value of approximately 0.36 mm/s assigned to Fe^{3+} in $3R^{2+}$ (arrangement referred to as A), and the doublet with Δ of approximately 0.6 mm/s assigned to Fe^{3+} in mixed-type arrangements $2R^{3+}1R^{2+}$ and $2R^{2+}1R^{3+}$ (referred to as K).

The computer program described and the integrated optical densities listed in column 5 of Table 1 were used to evaluate the expected intensities for Fe^{3+}-doublets. As b-oriented $R^{2+}R^{2+}$ pairs are absent (Table 1), the occurrence probability $W_{R^{2+}R^{2+}}$ equals 0 and the HDC principle is realized at the one-dimensional level. To analyze in what way the HDC principle may be realized at the two-dimensional level, at least two situations should be considered. The first is the "IR-pref." mode with R^{2+} cations situated, for example, only in the "left" cis-positions (with fixed b-direction). In this case, as was mentioned above, the HDC principle is automatically extended to the two-dimensional octahedral net, and the cation distribution with an imposed "segregation" limitation can be analysed if the penalty function parameter α equals 1. The second case is the "IR-equiv." mode. Here, either HDC limitation ($\alpha = 0$), or both HDC and "segregation" limitation ($\alpha = 0.5$) may be imposed. Table 2 represents integrated optical densities for celadonite-like domains (column 5 of Table 1) given as a matrix of occurrence probabilities of cation pairs in adjacent cis-octahedra linked through OH-groups. Matrix (a) corresponds to equivalence of cis-positions "I" and "II" with respect to occupancy by cations of distinct sorts. Matrix (b) corresponds to preference of R^{2+} cations for one of the cis-positions. Four extreme modes were chosen for synthetic spectra: "IR-equiv." and "IR-pref." for random distribution of cation pairs with relevant W_{ik} (matrix a and b of Table 2), and "IR-equiv., $\alpha = 0.5$, S = 3000," and "IR-pref., $\alpha = 1$, S = 3000". For these modes the occurrence probabilities W_A, W_F, and W_K for $3R^{2+}$-, $3R^{3+}$- and mixed-type arrangements $2R^{3+}1R^{2+}$ and $2R^{2+}1R^{3+}$ were calculated.

Supposing the equality of recoil-free fraction f' for considered structural Fe sites, the intensities of the expected doublets may be proportional to the corresponding calculated occurrence probabilities. Table 3 demonstrates the normalized intensities for the four analyzed modes of cation distribution. Relative weights for Fe^{2+}-doublets and a Fe^{3+}/Fe^{2+} ratio were determined from the experimental spectra. Isomer shifts for Fe^{3+}-doublets were assumed to be equal. The shift of the centre of gravity for Fe^{3+}-doublets with respect to the centre of gravity for Fe^{2+}-doublets was determined from the experimental spectra. The half-widths for all doublets were considered to be equal to 0.3 mm/s. The results of the synthesis are shown in Figure 3. Changes

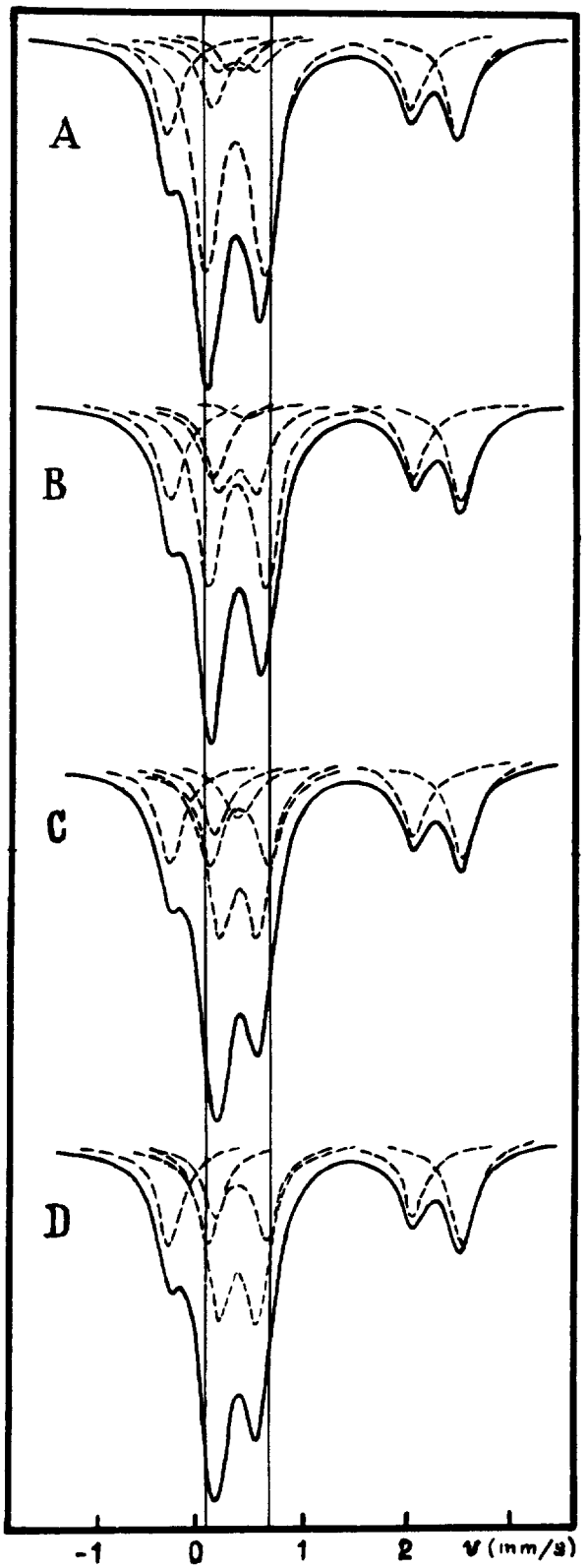

Figure 3. Computer synthesized Mössbauer spectra for glauconite *B. Patom*, line widths 0.3 mm/c. (A) "IR-equiv." mode, ← equivalence of cis-positions "I" and "II" with respect to cations of various types, random distribution of cation pairs with W_{ik} values from matrix (a) of Table 2; (B) "IR-equiv.", α = 0.5, S = 3000 mode, equivalence of cis-positions, both HDC and "segregation" limitations imposed, 3000 steps in the improvement procedure; (C) "IR-pref." mode, random distribution of cation pairs with W_{ik} values from matrix (b) of Table 2; (D) "IR-pref.", α = 1, S = 3000 mode, preference of R^{2+} cations to one of cis-positions, "segregation" limitation imposed, 3000 steps in the improvement procedure.

Table 3. Normalized intensities used to synthetize Mössbauer spectra of glauconite *B. Patom* for various cation distribution modes.

	Cation distribution mode			
Doublet	"IR-equiv."	"IR-equiv., α = 0.5, S = 3000"	"IR-pref."	"IR-pref., α = 1.0, S = 3000"
F	0.05	0.01	0.07	0.07
A	0.07	0.18	0.34	0.35
K	0.50	0.43	0.21	0.20
Fe^{2+}	0.22	0.22	0.22	0.22
Fe^{2+}	0.16	0.16	0.16	0.16

in the form of the spectra and the visual quadrupole splitting depend upon whether cis-positions "I" and "II" are equivalent with respect to occupancy by cations of various valencies and to a minor extent upon a discrimination of $R^{2+}R^{2+}$ and $AlFe^{3+}$ pairs oriented in the b_1 or b_2 directions. A closer approximation to the experimental spectrum (Figure 2) is achieved by using "IR-pref." modes. The decisive factor is the maximum relative intensity for the A doublet that corresponds to the maximum occurrence probability W_A for Fe^{3+}, with three nearest R^{2+} cations.

The synthesis parameters for "IR-pref." modes were used as the initial parameters for fitting the experimental spectrum. The only difference was that the possibility for the presence of a low intensity doublet with Δ of approximately 1.0 mm/s assigned to Fe^{3+} in dehydroxylated octahedra (see, for example, Dainyak 1985; Bowen *et al.*, 1989) was taken into account. The fitted parameters of the spectrum are shown in Figure 2 and in Table 4. The χ^2 for the fitting is 1.6. When the intervals for Δ and δ fitting parameters were rather narrow, the decrease in a number of doublets gave χ^2 a value of 7.8, or higher.

It follows from the Mössbauer parameters represented in Table 4 that the spectrum of the glauconite *B. Patom* can be formally fitted to the number of doublets with their Δ values and intensities corresponding to the suggested model. As the model was constructed for a hypothetical celadonite with a crystallo-chemical formula including about 65% of the glauconite *B. Patom,* it is worthwhile to evaluate whether a cation distribution showing a coexistence of celadonite-like and illite-like domains can be simulated for the glauconite studied.

https://doi.org/10.1346/CCMN.1992.0400412 Published online by Cambridge University Press

Table 4. Mössbauer parameters for glauconite *B. Patom* at room temperature ($\chi^2 = 1.6$)[1]

Doublet assignment	Δ (mm/s)	δ (mm/s)	Γ (mm/s)	%
Fe^{3+} [2] F	0.19	0.37	0.28	7.1
A	0.39	0.37	0.38	37.2
K	0.60	0.37	0.38	16.2
"x"	1.08	0.40	0.40	3.2
Fe^{2+}	2.82	1.14	0.30	14.8
Fe^{2+}	1.92	1.07	0.57	21.5

[1] Isomer shift δ vs. α-Fe, quadrupole splitting Δ, full width at half-maximum Γ and relative peak area %. Estimated errors are ±0.01 mm/s for δ and ±0.02 mm/s for Δ. Estimated error in % is ±3%.

[2] Cations Fe^{3+} occupy cis-positions only. Symbols F, A, and K denote the ($3R^{3+}$), ($3R^{2+}$) and ($1R^{2+}$ $2R^{3+}$, $1R^{3+}$ $2R^{2+}$) arrangements consisting of three octahedral cations nearest to the central Fe^{3+}. Symbol "x" stands for Fe^{3+} in dehydroxylated octahedra.

Computer simulation of the octahedral cation distribution in glauconite B. Patom

Here, the integrated optical densities of the component bands in the glauconite IR-spectrum (column I of Table 1) must be used as a starting point. As in the case for computer simulation of cation distribution in hypothetical celadonite, two possibilities for fulfilling the HDC-principle at the two-dimensional level should be considered. Table 5 represents integrated optical densities from column I of Table 1 given as a matrix of occurrence probabilities of cation pairs in adjacent cis-octahedra linked through OH-groups. Matrix (a) corresponds to equivalence of cis-positions "I" and "II," with respect to occupancy by cations of various sorts ("IR-equiv." mode). Matrix (b) corresponds to preference of R^{2+} cations to one of the cis-positions ("IR-pref." mode).

We analysed the occurrence probabilities W_A, W_F, and W_K for arrangements A, F, and K versus the occurrence probability $W_{Al\text{-}3Al}$ for "clustering" Al-3Al arrangement for both modes. The corresponding curves are shown in Figures 4A–C. The starting points (dashed verticals) for these dependences correspond to random distribution of cation pairs with relevant W_{IK} for each

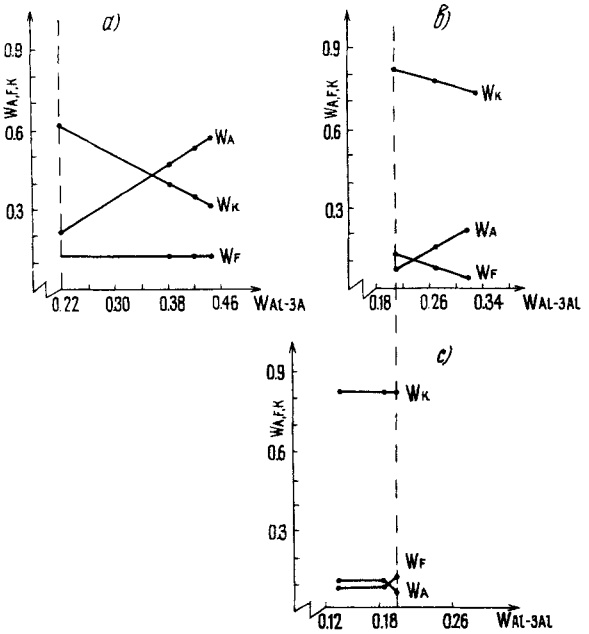

Figure 4. Occurrence probabilities W_A, W_F, and W_K versus occurrence probability $W_{Al\text{-}3Al}$ for cation distribution modes: (A) "IR-pref.", $\alpha = 1.0$; (B) "IR-equiv.", $\alpha = 0.5$; and (C) "IR-equiv.", $\alpha = 0.0$. The dashed vertical indicates points corresponding to random distribution of cation pairs with W_{ik} values (i, k = Mg, Fe^{2+}, Fe^{3+}, Al) derived from computer-resolved IR-spectra.

mode. Other points correspond to cation distributions with the minimum penalty function at the consecutive levels of the "improvement" procedure.

In "IR-equiv." mode, the suppression of both $AlFe^{3+}$ and $R^{2+}R^{2+}$ pairs in b_1, b_2 directions ($\alpha = 0.5$) does not yield considerable segregation: $W_{Al\text{-}3Al}$ value does not exceed 0.32 (Figures 4B and 4C), while its maximum value, as can be shown in the case of absolute segregation of Al, would be 0.57. The probability range of arrangements A, F, and K is rather narrow, with the K arrangement predominant. The situation radically changes in "IR-pref., $\alpha = 1$ mode (Figure 4A). The probability for Al-3Al arrangement varies from 0.22 to 0.44 so that for values exceeding 0.36 the A ar-

Table 5. Occurrence probabilities of cation pairs W_{ik} (i,k = Mg, Fe^{2+}, Fe^{3+}, Al) for the b direction (column 1 of Table 1) corresponding to: a) equivalence of cis-positions "I" and "II" with respect to cations of various types and b) preferential occupany of one of the positions by R^{2+} cations.

a						b					
	I						I				
II	Mg	Fe^{2+}	Fe^{3+}	Al	W_k	II	Mg	Fe^{2+}	Fe^{3+}	Al	W_k
Mg	0.0	0.0	0.03	0.13	0.17	Mg	0.0	0.0	0.0	0.0	0.0
Fe^{2+}	0.0	0.0	0.10	0.0	0.10	Fe^{2+}	0.0	0.0	0.0	0.0	0.0
Fe^{3+}	0.03	0.10	0.0	0.04	0.17	Fe^{3+}	0.07	0.20	0.0	0.04	0.31
Al	0.13	0.0	0.04	0.38	0.55	Al	0.27	0.0	0.04	0.38	0.69
W_i	0.17	0.10	0.17	0.55	1.0 1.0	W_i	0.34	0.20	0.04	0.42	1.0 1.0

https://doi.org/10.1346/CCMN.1992.0400412 Published online by Cambridge University Press

rangement becomes prevalent. The difference between the case of cis-position equivalency with respect to R^{2+} and R^{3+} occupancy and the case of R^{2+} preference to the one of cis-positions is well illustrated by the W_A, W_F, and W_K triangle (Figure 5).

Dispersion fields for probabilities corresponding to these cases do not overlap. The computer simulation has shown that with different W_A, W_F, and W_K sets the effectiveness of the penalty function with parameter $\alpha = 1.0$ for the "IR-pref." mode and with parameter $\alpha = 0.5$ for the "IR-equiv." mode is the same. No $R^{2+}R^{2+}$ pairs are present in b_1,b_2 directions, while the number of remaining $AlFe^{3+}$ pairs is almost the same. Two conclusions follow from this result. The first is that the HDC principle may be realized independent of preference or non-preference for R^{2+} cations for one of the cis-positions. The second is that imposing the principle of homogeneous dispersion of charges along with suppressing $AlFe^{3+}$ pairs is necessary, but not sufficient for the formation of more or less large domains. From the crystallo-chemical point of view, the decisive role here is played by non-equivalency of "left" and "right" cis-positions (with fixed b-direction) with respect to the R^{2+} and R^{3+} occupancy.

The mode of cation distribution "IR-pref., $\alpha = 1.0$, S = 3000" contains arrangements A, F, K whose occurrences are the closest to those obtained from the computer resolved Mössbauer spectrum. In fact, occurrence probabilities W_A, W_F, and W_K derived by normalizing the relevant areas under peaks A, F, and K to their total area in Mössbauer spectrum are equal to 0.61, 0.11 and 0.28, respectively. These probability values for the cation distribution mode are equal to 0.56, 0.12, and 0.32, respectively. A fragment of this mode is shown in Figure 6. The structure is divided into illite-like domains of two to three unit cells (encircled with a line) and celadonite-like domains of three to four unit cells.

DISCUSSION

The Mössbauer spectrum of the glauconite *B. Patom* conforms to the model for which the glauconite structure is composed of celadonite-like and illite-like domains. Non-equivalence of "I" and "II" cis-positions with respect to R^{2+} and R^{3+} occupancy is realised in celadonite-like domains. Moreover, a decisive role in formation of more or less large domains is played by this non-equivalency. It is noteworthy that such a concept of glauconite structure satisfies both IR-spectroscopy data characterizing one-dimensional cation distribution and Mössbauer spectroscopy results sensitive to local order-disorder at the two-dimensional level. The results also agree with the model of Townsend *et al.* (1987) for the interpretation of the ferromagnetic ordering at 1.3 K in glauconite. In their model, Fe^{3+} cations are distributed over cis-positions so as to maximize their mutual separation implying the ordered

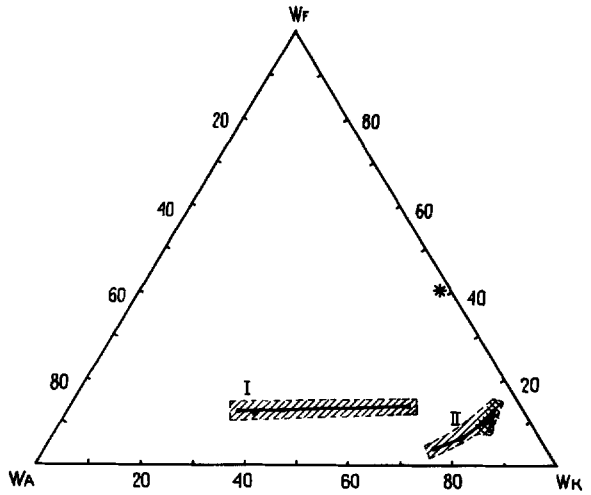

Figure 5. (W_A-W_F-W_K)-triangle: I—"IR-pref.", $\alpha = 1.0$ (▨); II—"IR-equiv.", $\alpha = 0.5$ (▨) and $\alpha = 0.0$ (■). Asterisk (*) stands for the point corresponding to random distribution of cations (but not of cation pairs).

alteration of Fe^{3+} in cis-positions, i.e., preference of Fe^{3+} to one of the positions. In addition, the transition to ferromagnetic ordering occurs within a certain temperature interval indicating an unhomogeneous structure. It is the domain structure of glauconite that causes this unhomogeneity.

The domain structure of glauconite may imply specific formation conditions which may interest geologists and mineralogists. However, the example considered does not cover all the diversity of natural

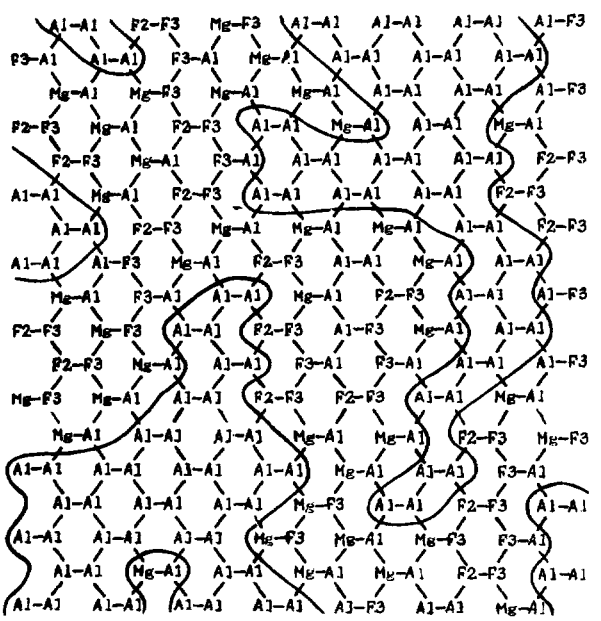

Figure 6. A portion of the octahedral sheet of glauconite, *B. Patom*, simulated under conditions "IR-pref.", $\alpha = 1.0$, S = 3000. Illite-like domains (Fe-free) are enclosed by a line. F3—Fe^{3+} cation, F2—Fe^{2+} cation.

https://doi.org/10.1346/CCMN.1992.0400412 Published online by Cambridge University Press

glauconites. In order to elucidate whether domain structure is wide-spread in glauconite, additional investigations are required. One may hope that Mössbauer spectroscopy will prove useful in this respect. The use of the computer program described is likely to promote the interpretation of the other glauconite spectra. It should be noted, however, that construction of a "hard" model for fitting the spectra also needs further improvement. This is especially true for EFG calculations for various nearest cation arrangements around Fe^{3+}.

Calculations of EFG for Zavalie celadonite, nontronite and Red muscovite based on structural modeling (Dainyak *et al.*, 1984a, 1984b, 1984c; Dainyak, 1985; Dainyak and Drits, 1987) have shown that the fairly wide range of Δ values corresponding to various cation arrangements around Fe^{3+} for the given structure is directly associated with the peculiarities in the shape of the Fe^{3+}-octahedra that depends on the nearest coordinating cations, and therefore differs from the octahedral shape in the averaged structure. At the same time, determination of the shape of an individual octahedron using structural modeling originates, to a considerable extent, from the average structure. This approach is justified by comparison of the Δ_{exp} and Δ_{cal} values for the nearest cation arrangements around Fe^{3+} that are identical with respect to cation valencies but differ in cation types, such as are present in distinct minerals. For example, ($3Fe^{3+}$) arrangement in Zavalie celadonite results in $\Delta_{exp} = \Delta_{cal} = 0.17$ mm/s while arrangement (3Al) in Red muscovite results in $\Delta_{exp} = 0.74$ mm/s and $\Delta_{cal} = 0.72$ mm/s (Dainyak and Drits, 1987). This correlates with the octahedral flattening angle, $\psi = \arccos \langle h_{oct} \rangle / 2d_{oct}$, where $\langle h_{oct} \rangle$ is the mean octahedral thickness and d_{oct} is the mean octahedral cation-anion distance. The ψ values for Zavalie celadonite and Red muscovite are 56.2° and 57.1° respectively.

Since the crystallo-chemical formula for hypothetical celadonite used in constructing the model differs from that of Zavalie celadonite, it is appropriate to evaluate the ψ value in hypothetical celadonite. Synthesized spectra shown in Figure 3 once again confirm the need to do this. If the whole range of ψ values for hypothetical celadonite is assumed to be shifted to the left along the velocity scale, then spectra shape for "IR-equiv." modes (Figures 3A and 3B) might be closer to that of the experimental spectrum. It is obvious that a totally different model would then be chosen for fitting the experimental spectrum. The recent achievements in structural modeling (Smoliar-Zviagina, 1991; Zviagina and Drits, 1991; Drits and Smoliar-Zviagina, 1992) allow estimation of ψ directly from the chemical composition of the hypothetical celadonite. Application of the regression equations of Smoliar-Zviagina (1991) yields $\psi = 56.6°$. This value implies that the Δ range may be shifted, if at all, only to the right along the velocity scale, indicating that the choice of the model is justified by the structural features of the hypothetical celadonite. Since, however, not all glauconite spectra contain prompts indicating the presence of celadonite-like domains, special EFG calculations can hardly be avoided in the future.

Among other features of the fitting presented in Figure 2 and Table 4, note the Fe^{3+}-doublet with $\Delta = 1.08$ mm/s denoted as "x" that might correspond to Fe^{3+} in dehydroxylated octahedra. Since the intensity of this doublet is low, its presence can be treated as an artifact resulting from the fitting with Lorentzian peak lineshapes.

The nature of two Fe^{2+}-doublets will not be analyzed in this paper. We note, however, that consideration of nearest-neighbour cations arrangements is appropriate not only for Fe^{3+}, but for Fe^{2+} also.

ACKNOWLEDGMENTS

The authors are grateful to Mr. Yu. G. Belostotsky who translated the text, to Dr. D. D. Eberl for corrections of the English and to Mrs. B. Smoliar-Zviagina for valuable comments.

REFERENCES

Besson, G., Bookin, A. S., Dainyak, L. G., Rautureau, M., Tsipursky, S. I., Tchoubar, C., and Drits, V. A. (1983) Use of diffraction and Mössbauer methods for the structural and crystallochemical characterization of nontronite: *J. Appl. Cryst.* **16,** 374–383.

Besson, G., Drits, V. A., Dainyak, L. G., and Smoliar, B. B. (1987) Analysis of cation distribution in dioctahedral micaceous minerals on the basis of IR-spectroscopy data: *Clay Miner.* **22,** 465–478.

Bookin, A. S., Dainyak, L. G., and Drits, V. A. (1978) Interpretation of the Mössbauer spectra of layer silicates on the basis of structural modelling (c): *Phys. Chem. Minerals.* **3,** 58–59.

Bowen, L. H., De Grave, E., Reid, D. A., Graham, R. C., and Edinger, S. B. (1989) Mössbauer study of a California desert celadonite and its pedagenically-related smectite: *Phys. Chem. Minerals,* **16,** 697–703.

Cardile, C. M. and Brown, I. N. M. (1988) An ^{57}Fe Mössbauer and X-ray diffraction study of New Zealand glauconites: *Clay Miner.* **23,** 13–25.

Dainyak, L. G. (1985) Structural features of layer silicates and EFG calculations for an interpretation of their Mössbauer spectra: in *Proc. 5th Meeting of the European Clay Groups, Prague, 1983,* J. Konta, ed., Univerzita Karlova, Prague, 43–49.

Dainyak, L. G. and Drits, V. A. (1987) Interpretation of Mössbauer spectra of nontronite celadonite and glauconite: *Clays & Clay Minerals* **35,** 363–372.

Dainyak, L. G., Bookin, A. S., and Drits, V. A. (1984a) Interpretation of Mössbauer spectra of dioctahedral Fe^{3+}-containing 2:1 layer silicates. II. Nontronite: *Kristallografia* **29,** 304–311 (in Russian).

Dainyak, L. G., Bookin, A. S., and Drits, V. A. (1984b) Interpretation of Mössbauer spectra of dioctahedral Fe^{3+}-containing 2:1 layer silicates. III. Celadonite: *Kristallografia* **29,** 312–321 (in Russian).

Dainyak, L. G., Dainyak, B. A., Bookin, A. S., and Drits, V. A. (1984c) Interpretation of the Mössbauer spectra of

dioctahedral Fe^{3+}-containing layer silicates on the basis of structural modelling: *Kristallografia* **29,** 94–100 (in Russian).

De Grave, E., Vandenbruwaene, J., and Elewaute, E. (1985) An ^{57}Fe Mössbauer effect study on glauconites from different locations in Belgium and northern France: *Clay Miner.* **20,** 171–179.

Drits, V. A. and Smoliar-Zviagina, B. B. (1992) Structure prediction for micas of diverse compositions: (submitted to *Zeitchrift für Kristallographie*).

Drits, V. A., Kameneva, M. Y., Sakharov, B. A., Dainyak, L. G. (1992) Problems in the determination of the actual structure of glauconite and related microdivided minerals: in *Nauka,* Inst. Geol. Geophys. Soran, Novosobirsk, 360 pp. (in Russian).

Herrero, C. P., Gregorkievitz, M., Sanz, J., and Serratoza, J. M. (1987) ^{29}Si MAS-NMR spectroscopy of mica-type silicates: Observed and predicted distribution of tetrahedral Al-Si: *Phys. Chem. Minerals* **15,** 84–90.

Johnston, J. H. and Cardile, C. M. (1987) Iron substitution in montmorillonite, illite, and glauconite by ^{57}Fe Mössbauer spectroscopy: *Clays & Clay Minerals* **35,** 170–176.

Kameneva, M. Y. (1986). Crystal-chemical peculiarities of the glauconite group minerals: Ph.D. thesis, Inst. Geol. Geophys. Soran, Novosobirsk (in Russian).

Krzanowski, W. J. and Newman, A. C. D. (1972) Computer simulation of cation distribution in the octahedral layers of micas: *Mineral. Mag.* **38,** 926–935.

Lippmaa, E., Magi, M., Samoson, A., Engelhardt, G., and Grimmer, A. R. (1980) Structural studies of silicates by solid-state high resolution ^{29}Si NMR: *J. Amer. Chem. Soc.* **102,** 4889–4893.

Nikolaeva, I. V. (1977) Minerals of the glauconite group in sedimentary formations: in *Nauka,* Moscow, 321 pp. (in Russian).

Popov, V. I., Khramov, D. A., and Lobanov, F. I. (1988) Absorber shape: The influence on the Mössbauer spectrum parameters: in *Proc. of USSR Conference on Applied Mössbauer Spectroscopy "Volga",* Moscow Physical Engineering Inst., Moscow, 32–33 (in Russian).

Sakharov, B. A., Besson, G., Drits, V. A., Kameneva, M. Y., Salyn, A. L., and Smoliar, B. B. (1990) X-ray study of the nature of stacking faults in the structure of glauconites: *Clay Miner.* **25,** 419–435.

Sanz, J. and Serratoza, J. M. (1984) ^{29}Si and ^{27}Al high-resolution MAS-NMR spectra of phyllosilicates: *J. Amer. Chem. Soc.* **106,** 4790–4793.

Slonimskaya, M. V., Besson, G., Dainyak, L. G., Tchoubar, C., and Drits, V. A. (1986) Interpretation of the IR spectra of celadonites and glauconites in the region of OH-stretching frequencies: *Clay Miner.* **21,** 377–388.

Smoliar-Zviagina, B. B. (1991) Relationships between structural parameters and chemical composition of 2:1 phyllosilicates: in *Proc. Euroclay Conference, Dresden, 1991,* M. Storr, K.-H. Henning, and P. Adolphi, eds., Ernst-Moritz-Universitat, Greifswald 3, 975–980.

Townsend, M. G., Longworth, G., Ross, C. A. M., and Provencher, R. (1987) Ferromagnetic or antiferromagnetic Fe III spin configurations in sheet silicates: *Phys. Chem. Minerals* **15,** 64–70.

Tsipursky, S. I. and Drits, V. A. (1984) The distribution of octahedral cations in the 2:1 layers of dioctahedral smectites: *Clay Miner.* **19,** 177–193.

Tsipursky, S. I., Drits, V. A., and Chekin, S. S. (1978) Study of structural ordering of nontronite by means of oblique electron diffraction: *Izv. Akad. Nauk S.S.S.R., Ser. Geol.* **10,** 105–113 (in Russian).

Tsipursky, S. I., Drits, V. A., and Plançon, A. (1985) Calculation of the intensities distribution in the oblique texture electron diffraction patterns: *Kristallografia* **30,** 38–44 (in Russian).

Zviagina, B. B. and Drits, V. A. (1991) Structure modelling of micas having disordered distribution of isomorphous cations: *Miner. Zhurnal* **13,** 84–95 (in Russian).

(Received 13 May 1992; accepted 8 June 1992; Ms. 2134)